

Violent White Dwarf Mergers or Collisions Produce Type Ia Supernovae in Elliptical Galaxies

MICHAEL A. TUCKER^{1,2,*}

¹*Center for Cosmology and AstroParticle Physics, 191 W Woodruff Ave, Columbus, OH 43210*

²*Department of Astronomy, The Ohio State University, 140 W 18th Ave, Columbus, OH 43210*

Submitted to ApJL

ABSTRACT

I find that Type Ia supernovae (SNe Ia) with bimodal nebular emission profiles occur almost exclusively in massive ($M_\star \gtrsim 10^{11} M_\odot$) galaxies with low star-formation rates ($SFR \lesssim 0.5 M_\odot/\text{yr}$). The bimodal profiles are likely produced by two white dwarfs that exploded during a merger or collision, supported by a correlation between the peak-to-peak velocity separation (v_{sep}) and the SN Ia peak luminosity (M_V) which arises naturally from more massive white dwarf binaries synthesizing more ^{56}Ni during the explosion. The quiescent hosts are consistent with the long delay times required to form double white dwarf binaries. The distributions of SNe Ia with and without bimodal nebular lines differ in host mass, SFR, and specific SFR with K-S test probabilities of 3.1%, 0.03%, and 0.02%, respectively. Viewing angle effects can fully explain the SNe Ia in quiescent hosts without bimodal emission profiles and the dearth of merger/collision driven SNe Ia in star-forming hosts requires at least two distinct progenitor channels for SNe Ia. 30–40% of all SNe Ia originate from mergers or collisions depending on how cleanly host environment distinguishes progenitor scenarios. The bimodal SNe Ia share some characteristics with the underluminous 91bg-like SNe Ia that also prefer older populations, but there is no unambiguous connection between the two classifications. This may suggest separate processes or multiple axes of ejecta (a)symmetry. Existing models for WD mergers and collisions broadly reproduce the $v_{\text{sep}} - M_V$ correlation and future analyses may be able to infer the masses/mass-ratios of merging white dwarfs in external galaxies.

Keywords: Type Ia supernovae (1728), White dwarf stars (1799), Stellar mergers (2157), Elliptical galaxies (456)

1. INTRODUCTION

Type Ia supernovae (SNe Ia) are the thermonuclear explosion of white dwarf (WD) stars (Hoyle & Fowler 1960). Since WDs do not spontaneously ignite, a companion is needed to destabilize the WD. The nature of the companion has been the source of extensive debate (see Maoz et al. 2014 and Jha et al. 2019 for reviews). SNe Ia also produce the majority of iron-group elements in the Universe (Iwamoto et al. 1999; Kobayashi et al. 2020) and the exact nucleosynthetic yields depend sensitively on the density and chemical composition of the core (e.g., Seitenzahl et al. 2013; Boos et al. 2021; Gronow et al. 2021), which in turns depends on how the WD explodes as a SN Ia.

Progenitors are generally divided into 2 categories depending on the nature of the companion. The single-degenerate (SD) scenario invokes a non-degenerate companion such as a main-sequence or red giant star (Whelan & Iben 1973; Nomoto 1982), whereas the double-degenerate (DD) scenario has a second WD as the companion star (e.g., Tutukov & Yungelson 1979; Iben & Tutukov 1984). The SD scenario predicts several observational signatures from the SN ejecta interacting with the companion (e.g., Wheeler et al. 1975; Marietta et al. 2000; Kasen 2010; Boehner et al. 2017) or its wind (e.g., Panagia et al. 2006; Margutti et al. 2012). Searches for these signatures consistently produce null results (e.g., Mattila et al. 2005; Leonard 2007; Schaefer & Pagnotta 2012; Shappee & Thompson 2013; Chomiuk et al. 2016; Maguire et al. 2016; Tucker et al. 2020; Dubay et al.

* CCAPP Fellow

2022; Tucker & Shappee 2024, see Liu et al. 2023a for a review).

The non-detections of SD companions implies that double-WD binaries produce most SNe Ia. The question becomes *how* the two WDs evolve to a detonation. Gravitational-wave emission and tidal forces can slowly reduce the orbital separation until mass-transfer or disruption occurs (e.g., Carvalho et al. 2022). Mergers can explode during coalescence ('violent' mergers; e.g., Pakmor et al. 2010, 2012, 2013) or after some time delay spanning $\sim 10^2 - 10^6$ years (e.g., Ji et al. 2013; Becerra et al. 2018; Neopane et al. 2022). Dynamics in triple- and quadruple-star systems can induce mergers or even direct collisions (Thompson 2011; Shappee & Thompson 2013; Pejcha et al. 2013; Antognini et al. 2014; Fang et al. 2018; Hamers et al. 2022) but these scenarios struggle to reproduce the total SN Ia rate (e.g., Toonen et al. 2018; Hamers 2018). Double detonations in double-WD binaries (e.g., Livne 1990; Shen & Moore 2014) show promise for reproducing normal SNe Ia (e.g., Shen et al. 2018; Polin et al. 2019), but current models over-predict the diversity of SN Ia light curves (e.g., Shen et al. 2021; Collins et al. 2022).

Host-galaxy and environmental analyses, which indirectly trace SN Ia progenitors, consistently find a diversity of explosion sites (e.g., Hakobyan et al. 2020; Cronin et al. 2021). There are correlations between the local environment and SN properties (Childress et al. 2013; Pan et al. 2015; Meng et al. 2023) but the underlying origin is unknown. Accounting for these effects in cosmological analyses remains empirical (e.g., the 'mass-step' correction, Kelly et al. 2010; Sullivan et al. 2010) and recent analyses suggest distinct progenitors in young and old stellar populations (e.g., Wang et al. 2013; Rigault et al. 2020) with a $\sim 0.1 - 0.2$ mag intrinsic luminosity difference (Briday et al. 2022).

Yet connecting these environmental correlations to intrinsic ignition conditions or progenitor systems has proven difficult, primarily due to the explosion physics inherent to SNe Ia. Exploding a $\sim 1 M_{\odot}$ star comprised of carbon and oxygen naturally produces a bright transient and layered ejecta with iron-group elements in the core surrounded by intermediate-mass elements from incomplete Si-burning (Seitenzahl & Townsley 2017). Sky surveys and follow-up programs have obtained light curves and spectra for hundreds of SNe Ia in the weeks around maximum light (e.g., Blondin et al. 2012; Silverman et al. 2012a; Morrell et al. 2024) but these observations only probe the outer ejecta (e.g., Mazzali et al. 2014).

Nebular-phase spectra, obtained $\gtrsim 200$ days after explosion when the ejecta becomes optically thin, provide

a direct view to the central regions of the explosion. These spectra are dominated by high-velocity forbidden emission lines from iron-group elements (Co, Ni, Fe; e.g., Wilk et al. 2020; Kwok et al. 2023) heated by radioactive-decay energy (Seitenzahl et al. 2009). Most nebular spectra show smooth emission-line profiles (e.g., Maguire et al. 2018) with correlations between early-time and late-time ejecta velocities suggesting minor ejecta asymmetries (e.g., Maeda et al. 2010; Liu et al. 2023b). Yet Dong et al. (2015) discovered a subset of SNe Ia that show significantly asymmetric, even bimodal or double-peaked, nebular emission lines. Vallely et al. (2020) later used an expanded sample to show that the SNe Ia with bimodal profiles have below-average luminosities but otherwise resemble spectroscopically-normal SNe Ia.

In this Letter I connect these bimodal SNe Ia to exclusively old stellar populations. Moreover, the peak-to-peak velocity separation of the nebular profiles correlates with peak luminosity, a key prediction for WD mergers or collisions because total binary mass M_{tot} corresponds to faster orbital velocities and more synthesized ^{56}Ni . I outline the sample of SNe Ia searched for bimodality in §2. Bimodal nebular profiles are connected to host-galaxy mass and star-formation rate (SFR) in §3 and I discuss these findings in the context of SNe Ia and their progenitors in §4.

2. THE SAMPLE

Dong et al. (2015) and Vallely et al. (2020) conducted dedicated searches for SNe Ia with bimodal nebular profiles which I use as an initial sample. Those works searched for bimodality in 48 SNe Ia using new and archival nebular spectra. The SNe Ia are classified as 'bimodal' if the two velocity components are separated by more than their combined width (cf. Table 4 in Vallely et al. 2020). Table 1 provides the basic SN and host-galaxy properties for the sample.

There are 6 SNe Ia from in this sample that show bimodality in all three spectral features considered: the $[\text{Fe II}]$ blend at $\approx 5300 \text{ \AA}$, the isolated $[\text{Co III}] \lambda 5891$ line, and the $[\text{Fe II}] + [\text{Co III}]$ blend at $\approx 6600 \text{ \AA}$. Fig. 1 shows the nebular spectrum of SN 2007on (Gall et al. 2018; Mazzali et al. 2018) with bimodality in all three features. Included for comparison is the nebular spectrum of SN 2012cg (Silverman et al. 2012b; Shappee et al. 2018; Chakradhari et al. 2019) at a similar phase which is classified as 'not bimodal'.

There are 3 additional SNe Ia for which I retain the 'tentative bimodal' classification from Vallely et al. (2020). Two of these SNe Ia (2002er and 2016iuh) only show bimodal signatures in the $[\text{Co III}] \lambda 5891$ feature.

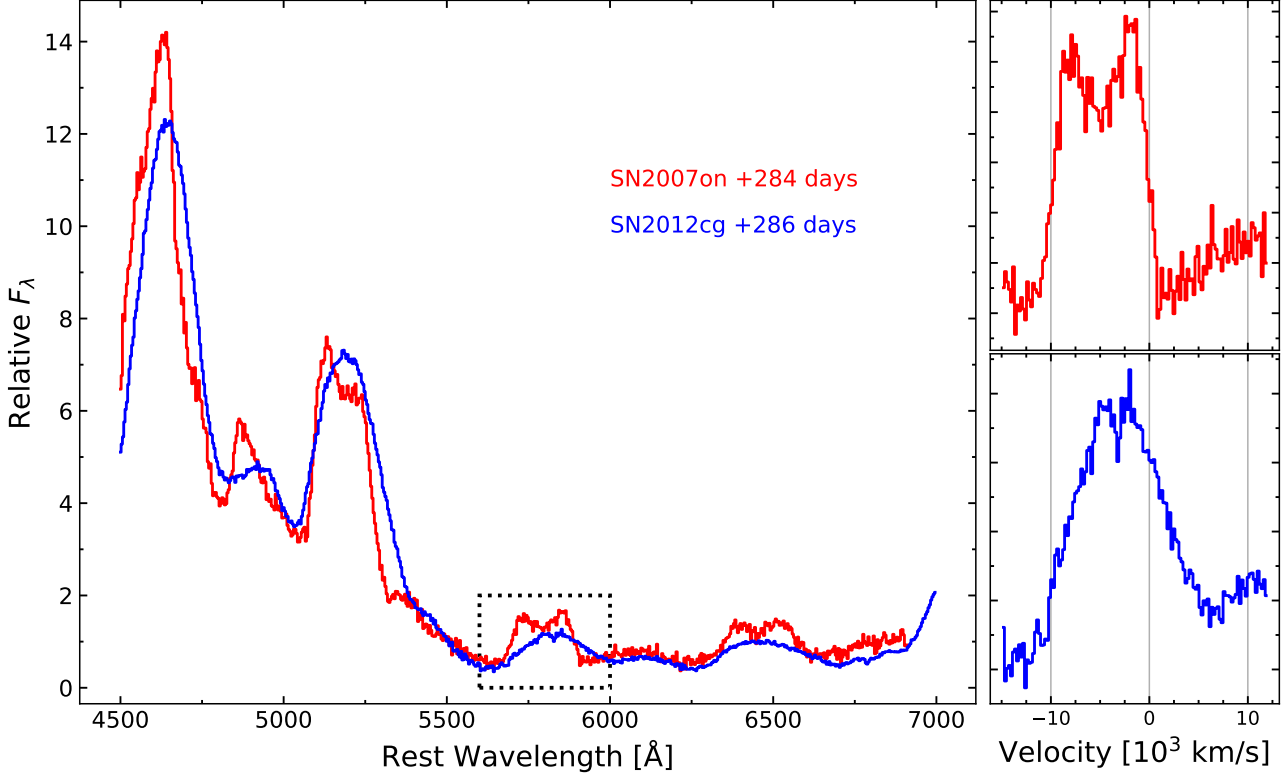


Figure 1. Example nebular spectra for SNe Ia with (SN 2007on, red) and without (SN 2012cg, blue) bimodal profiles. The dotted box marks the isolated [Co III] $\lambda 5891$ feature shown in velocity space in the right panels.

The spectra for these SNe Ia were obtained earlier in the nebular phase (+214 and +164 days, respectively) compared to the SNe Ia with bimodality detected in all three features (phases $\sim 250 - 350$ days). ^{56}Co decays to ^{56}Fe with a half-life of ≈ 77 days so these differences may simply trace the conversion of Co into Fe.

The third ‘tentative bimodal’ SN Ia, 1986G, is more likely to be a contamination artifact than SNe 2002er and 2016iuu. This explosion suffered from significant host-galaxy extinction and the host Na I absorption doublet falls atop the [Co III] $\lambda 5891$ feature. The redder [Fe II] +[Co III] feature also shows a strong absorption feature that might be due to over-subtraction of host-galaxy H α emission. Yet SN 1986G has similar properties to the other bimodal SNe Ia so I retain the ‘tentative bimodal’ classification. All three of these SNe Ia have open markers in the corresponding figures.

Finally, I add the 5 SNe Ia with nebular spectra from Graham et al. (2022) who searched for bimodality but did not find any detections. The combined sample from these 3 sources consists of 53 SNe Ia, 6 of which are confidently bimodal, three are tentatively bimodal, and the remaining 44 SNe Ia show no evidence for bimodal line profiles.

The full sample spans a wide range of near-peak photometric and spectroscopic properties (cf. Fig. 7 in Valleyly et al. 2020). Most of them are spectroscopically normal but there are 5 underluminous 91bg-like (Filippenko et al. 1992a; Leibundgut et al. 1993) and 5 overluminous 91T/99aa-like (Filippenko et al. 1992b; Phillips et al. 1992; Garavini et al. 2004), denoted with specific symbols in the corresponding figures. The 02cx-like/Iax SNe Ia (Li et al. 2003; Foley et al. 2013) are excluded as they likely originate from a different progenitor class and appear to never enter a true nebular phase (e.g., Foley et al. 2016; Camacho-Neves et al. 2023).

3. HOST GALAXIES

I compare the SNe Ia with and without bimodality to the stellar masses (M_\star), star-formation rates (SFR), and specific SFR ($\text{sSFR} = \text{SFR} / M_\star$) of their hosts. Most hosts have M_\star and SFR measurements in the ‘ $z = 0$ Multi-wavelength Galaxy Synthesis’ (z0MGS; Leroy et al. 2019) catalog anchored to $\sim 700,000$ galaxies in the GALEX-SDSS-WISE Legacy Catalog (GSWLC; Salim et al. 2016). Hosts for 4 of the SNe Ia in our sample are not included in z0MGS so we apply the same calibrations from Leroy et al. (2019) to the GALEX and WISE photometry for these hosts to ensure consistency.

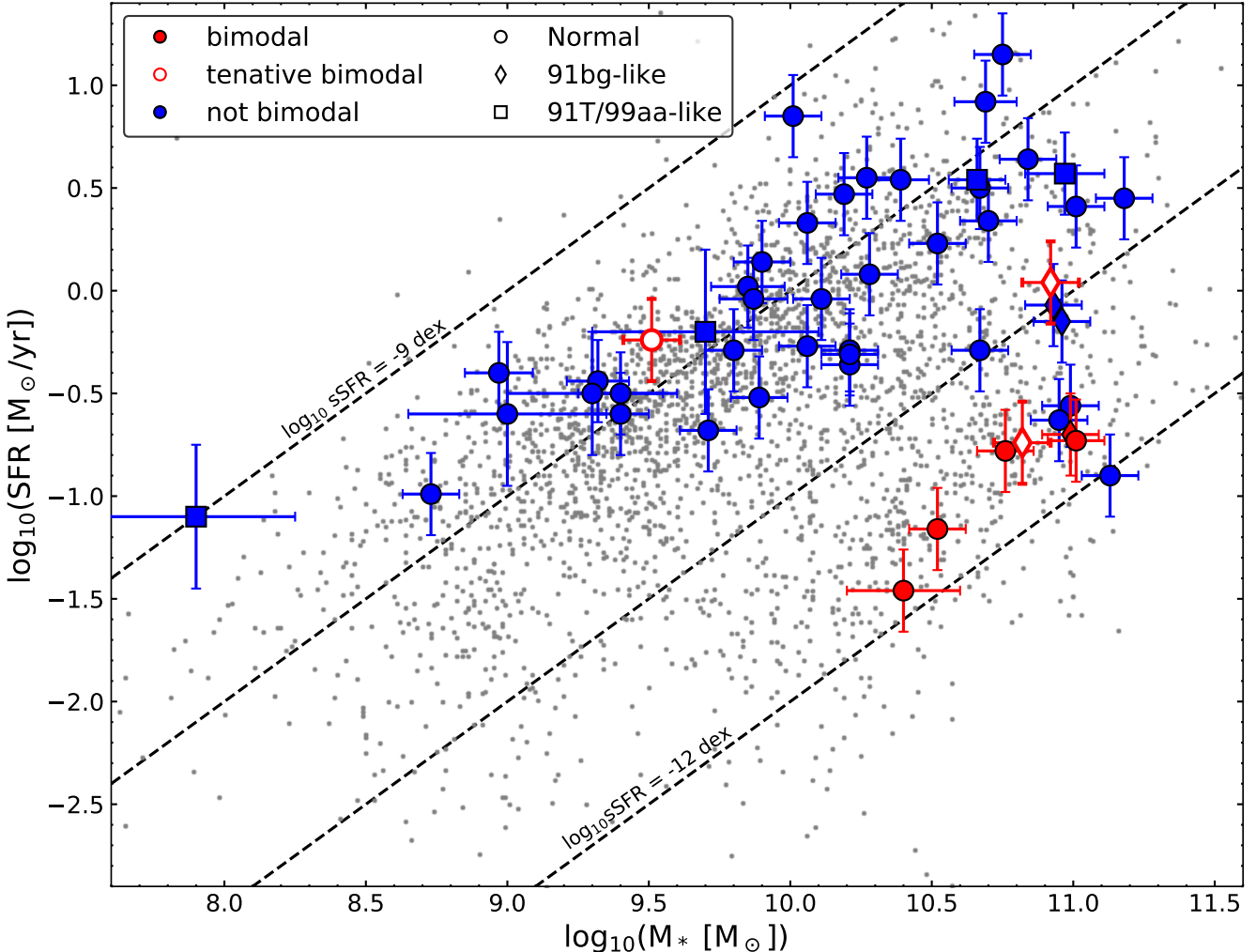


Figure 2. The host-galaxy masses and SFRs of bimodal SNe Ia (red) are compared to SNe Ia without bimodal nebular lines (blue). One host, NGC 1404, had 2 bimodal SNe Ia (2007on and 2011iv). Small grey points show a subset of galaxies from the z0MGS catalog (Leroy et al. 2019) for reference. The bimodal SNe Ia strongly prefer massive quiescent hosts.

Simply excluding these 4 SNe Ia, all of which are classified as ‘not bimodal’ and explode in star-forming hosts, does not affect the conclusions.

Fig. 2 shows the galaxy masses and SFRs for the SN Ia hosts color-coded by bimodality. The bimodal SNe Ia occur almost exclusively in massive ($\log_{10} M_* \simeq 11$ dex), quiescent ($\log_{10} \text{SFR} \lesssim -0.5$ dex) galaxies. The exception is the tentatively bimodal SN 2002er which occurs in a star-forming host. Two of the bimodal SNe Ia, SNe 2007on and 2011iv, share the same host galaxy NGC 1404.

I use the Kolmogorov-Smirnov (K-S) test to quantify whether the host properties of bimodal and non-bimodal SNe Ia differ. Fig. 3 shows the cumulative distribution functions (CDFs) for $\log_{10} M_*$, $\log_{10} \text{SFR}$, and $\log_{10} \text{sSFR}$ including the corresponding K-S p -values. The SFR and sSFR distributions in particular show

that the null hypotheses of no correlation between host-galaxy property and bimodality can be rejected at $> 99.9\%$ confidence. Leroy et al. (2019) note that their calibrations for SFR (and thus sSFR) likely overestimate the true values for passive galaxies ($\log_{10} \text{sSFR} \lesssim -11$ dex) because star-forming galaxies dominate their calibration sample. Reducing the SFR for these galaxies would further separate the bimodal SNe Ia from the majority of SN Ia hosts.

The presence of SNe Ia without bimodal profiles in these massive ellipticals agrees with viewing-angle effects obscuring asymmetry in some systems. If I just consider SNe Ia with hosts within 1σ of $\log_{10} \text{sSFR} \leq -11$ dex, $P_{\text{bm}} = 8/14$ (57%) of these SNe Ia show bimodal profiles. The observed fraction of bimodal SNe Ia P_{bm} is related to the critical viewing angle by

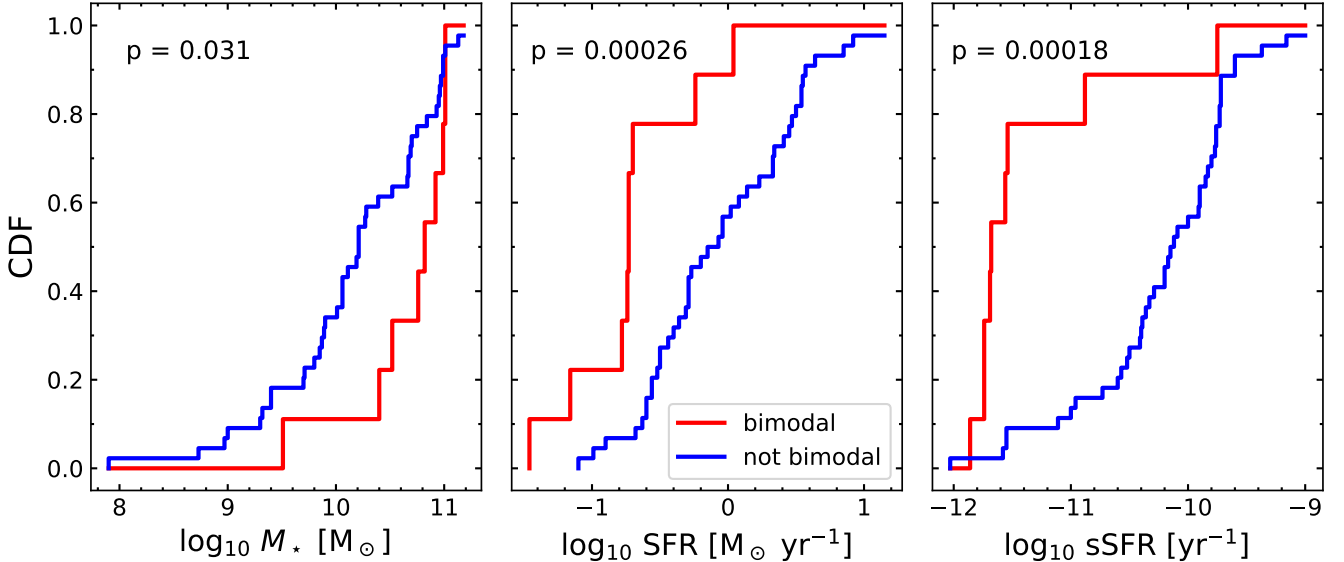


Figure 3. Cumulative distribution functions (CDFs) for SNe Ia with (red) and without (blue) bimodal nebular profiles. I show M_* (left), SFR (middle), and sSFR (right) including the p -value from the K-S test. The null hypotheses (the distributions are drawn from the same parent populations) can be rejected at the 99.9% level for SFR and sSFR.

$$\theta_c = 90^\circ - \cos^{-1}(P_{\text{bim}}/f), \quad (1)$$

where f is the ‘true’ fraction of bimodal SNe Ia. Explosions from violent mergers and collisions are expected to exhibit strong asymmetries, especially in the inner ejecta probed by the nebular Fe and Co features (e.g., Pakmor et al. 2013; Dong et al. 2015). For $f \equiv 1$, $\theta_c \simeq 35^\circ$, and this requires that most, if not all, SNe Ia in $\log_{10} \text{sSFR} \lesssim -11$ dex galaxies are intrinsically bimodal. However, the ‘tentative bimodal’ SN 2002er occurs in a host along the star-forming sequence which suggests some overlap between progenitor scenarios (see, e.g., Briday et al. 2022).

The separation by host sSFR allows a relatively clean estimate of the true fraction of all SNe Ia originating from collisions or mergers. Of the SNe Ia in my sample, 9/53 ($\simeq 17\%$) show evidence for bimodality and accounting for the \sim half that will not be classified as bimodal due to viewing-angle effects raises this fraction to $\sim 34\%$. SNe Ia in quiescent galaxies, including bimodal SNe Ia, are systematically fainter (e.g., Kelly et al. 2010; Sullivan et al. 2010; Gupta et al. 2011; Rigault et al. 2013) so there is likely some bias against late-time spectra for these events. For comparison, $\sim 35 - 40\%$ of the SN Ia hosts analyzed by Rigault et al. (2020) have $\log_{10} \text{sSFR} \lesssim -11$ dex although stellar population does not perfectly separate the two populations (Briday et al. 2022). With these considerations in mind, the intrinsic fraction of bimodal SNe Ia relative to all SNe Ia is probably 30–40%.

Finally, I do not find an unambiguous connection to the spectroscopic 91bg-like subclass of SNe Ia (diamonds in Fig. 2), which also have below-average peak luminosities (e.g., Filippenko et al. 1992a; Taubenberger et al. 2008; Hachinger et al. 2009) and a strong preference for passive hosts (e.g., Barkhudaryan et al. 2019). If 91bg-like classification is inclination dependent similar to bimodality, we would expect consistency between the bimodal and 91bg-like classifications. Common symmetry axes would produce correlated outcomes (bimodal \Leftrightarrow 91bg-like) whereas orthogonal axes would produce an anti-correlation (bimodal \neq 91bg-like). Neither of these are observed, as Fig. 2 shows all 4 possible combinations of these categories. Either there are different axes of symmetry between the inner and outer ejecta or different physical processes divide these empirical categories (e.g., Dhawan et al. 2017).

4. IMPLICATIONS FOR SN IA PROGENITORS

The dependence on sSFR explains correlations between SNe Ia and their hosts discovered over the past decade including the ‘step-correction’ parameterized by host mass, SFR, or sSFR. (e.g., Kelly et al. 2010; Sullivan et al. 2010; Lampeitl et al. 2010; Smith et al. 2012; Wang et al. 2013; Pan et al. 2014; Roman et al. 2018; Rigault et al. 2020; Kang et al. 2020; Kelsey et al. 2021; Briday et al. 2022; Wiseman et al. 2022, 2023; Larison et al. 2024; Ginolini et al. 2024). Valley et al. (2020) find that bimodal SNe Ia are $\delta m \sim 0.3$ mag fainter than the population average, slightly higher than the $\delta m \sim 0.2$ mag offset inferred by Briday et al. (2022)

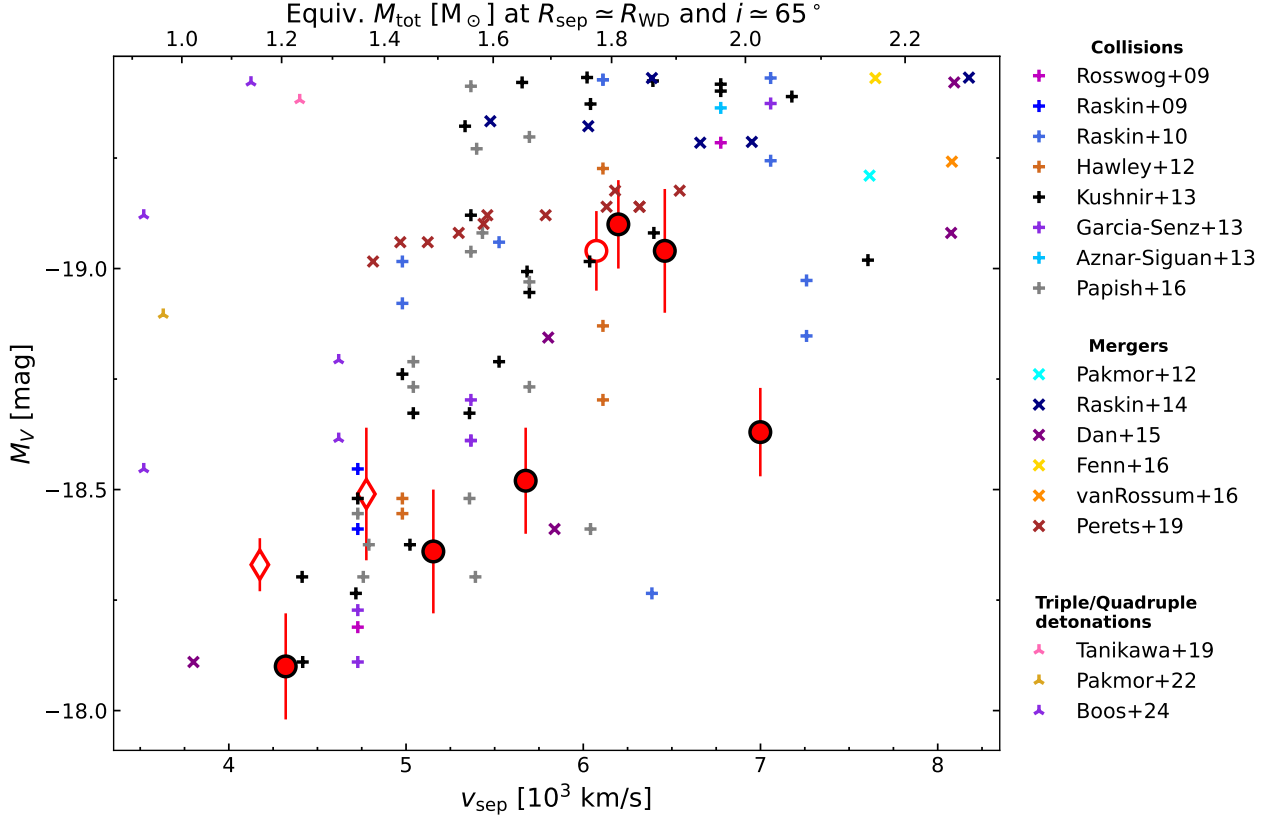


Figure 4. Correlation between the bimodal peak-to-peak velocity separation v_{sep} and peak V -band magnitude. Observations have the same markers and colors as in Fig. 2. The top axis shows the total binary mass if $v_{\text{orb}} \sim 1.1 \times v_{\text{sep}}$ corresponding to an average inclination of $i \simeq 65^\circ$. I use the synthesized $M_{^{56}\text{Ni}}$ to estimate M_V for models where two WDs explode, including collisions (+, Rosswog et al. 2009; Raskin et al. 2009, 2010; Hawley et al. 2012; Kushnir et al. 2013; García-Senz et al. 2013; Aznar-Siguán et al. 2013; Papish & Perets 2016), mergers (\times ; Pakmor et al. 2012; Raskin et al. 2014; Dan et al. 2015; Fenn et al. 2016; van Rossum et al. 2016; Perets et al. 2019), and triple- or quadruple-detonations (λ , Tanikawa et al. 2019; Pakmor et al. 2022; Boos et al. 2024). See §4 for details.

from a large sample of SNe Ia and host-galaxy properties. Yet the bimodal SNe Ia already have at least one axis of asymmetry so viewing-angle effects may account for the slightly larger δm calculated by Vallely et al. (2020) if luminosity and inclination are correlated.

The ^{56}Ni velocities exceed pre-explosion turbulent motions in the WD ($\sim 100 \text{ km s}^{-1}$; Höflich & Stein 2002; Kim et al. 2013) and the prevalence for roughly equal-height peaks in the bimodal profiles also disfavors internal explosive asymmetries such as deflagration plumes (e.g., Seitenzahl et al. 2013) or off-center detonations (e.g., Chamulak et al. 2012). Instead, multi-dimensional simulations of violent mergers (Pakmor et al. 2013) and collisions (Rosswog et al. 2009) show the highly-asymmetric ^{56}Ni distributions required by the bimodal line profiles.

The correlation between the peak-to-peak velocity separation v_{sep} and peak V -band magnitude M_V shown in Fig. 4 further suggests a collision or merger origin,

where v_{sep} measures the separation between the two velocity components in the nebular spectra and M_V is a reliable proxy for the bolometric luminosity (e.g., Arnett 1982). The Spearman correlation coefficient for v_{sep} and M_V in Fig. 4 is $r = -0.75$ with a statistically significant p -value of $p = 0.020$. The negative correlation coefficient corresponds to a *positive* correlation between v_{sep} and peak luminosity because the photometric magnitude system is inverted. This correlation is naturally produced if more massive WD binaries with faster orbits at contact synthesize more ^{56}Ni during the explosion, producing more radioactive decay power and brighter light curves.

The old stellar populations, bimodal nebular profiles, and $v_{\text{sep}} - M_V$ correlation are all consistent with the violent mergers or direct collisions of double-WD binaries. The top axis of Fig. 4 converts v_{sep} into an estimate for the total binary mass M_{tot} . The inclination angle i is unknown so I assume $v_{\text{orb}} \simeq 1.1 \times v_{\text{sep}}$ corresponding

to $i \approx 90 - \theta_c \simeq 65^\circ$. There is likely a slight observational bias towards identifying edge-on/high inclination systems.

I use the WD cooling tracks of Bédard et al. (2020) to estimate WD radii (R_{WD}) from their masses assuming thick H layers and a cooling age of 5 Gyr, although adopting anywhere between 1 – 10 Gyr produces similar results. To estimate M_V from $M_{56\text{Ni}}$ (a readily-provided quantity from most simulations), I combine the relation between the light curve ‘stretch’ parameter s_{BV} (Burns et al. 2011) and $M_{56\text{Ni}}$ from Scalzo et al. (2019) with the $s_{\text{BV}}-M_V$ calibration derived by Burns et al. (2018). This allows for direct comparison between models and observations even for simulations lacking radiative transfer computations.

Overall the collision and merger models agree well with the data in Fig. 4 assuming the separation at explosion is $R_{\text{sep}} \simeq (R_1 + R_2)/2$ (i.e., partially merged). Adopting different orbital separations at explosion moves the models horizontally in Fig. 4. Different viewing angles will likely shift the models along both axes because simulations suggest inclination-dependent light curves and spectra (e.g., Rosswog et al. 2009; Pakmor et al. 2012). Mergers must ignite during or soon after coalescence to produce the ^{56}Ni asymmetries, and any merger scenario must also reproduce the non-explosive merger remnants (e.g., Cheng et al. 2020; Kilic et al. 2021; Wu et al. 2022). Collisions depend on the impact parameter b where off-axis or grazing collisions reduce $M_{56\text{Ni}}$ or potentially prevent ignition altogether (e.g., Glanz et al. 2023).

The triple- and quadruple-detonation models (Papish et al. 2015) use a double-detonation on the primary to compress and ignite the secondary (triple detonations) or ignite a second double-detonation (quadruple detonations). These models have too low v_{sep} to match the data because they explode at larger separations, although this may depend on how the model binary is driven to explosion (Burmeister et al. 2023).

This rare electromagnetic observable to merging compact objects constrains key aspects of binary population synthesis models (e.g., Yungelson & Kuranov 2017), delay-time distributions (e.g., Maoz et al. 2010; Meng & Yang 2012), and the stochastic gravitational-wave background (e.g., Yu et al. 2020; Zou et al. 2020; Yoshida 2021). Many questions remain about how exactly the double WD binary is driven to explosion but these results confirm that violent mergers or collisions can and do produce spectroscopically-normal SNe Ia around maximum light. Moreover, this requires at least 2 separate progenitor channels for producing SNe Ia. The connection to host-galaxy sSFR allows for early identification of likely bimodal SNe Ia for detailed study.

Software: astropy (Astropy Collaboration et al. 2022); numpy (van der Walt et al. 2011; Harris et al. 2020); matplotlib (Hunter 2007); lmfit (Newville et al. 2014); scipy (Virtanen et al. 2020); spectres (Carnall 2017); emcee (Foreman-Mackey et al. 2013); pandas (The pandas development Team 2024)

ACKNOWLEDGMENTS

Many thanks to Adam Leroy, Chris Kochanek, Ben Shappee, and Kris Stanek for useful discussions.

REFERENCES

- Antognini, J. M., Shappee, B. J., Thompson, T. A., & Amaro-Seoane, P. 2014, MNRAS, 439, 1079, doi: [10.1093/mnras/stu039](https://doi.org/10.1093/mnras/stu039)
- Arnett, W. D. 1982, ApJ, 253, 785, doi: [10.1086/159681](https://doi.org/10.1086/159681)
- Astropy Collaboration, Price-Whelan, A. M., Lim, P. L., et al. 2022, ApJ, 935, 167, doi: [10.3847/1538-4357/ac7c74](https://doi.org/10.3847/1538-4357/ac7c74)
- Aznar-Siguán, G., García-Berro, E., Lorén-Aguilar, P., José, J., & Isern, J. 2013, MNRAS, 434, 2539, doi: [10.1093/mnras/stt1198](https://doi.org/10.1093/mnras/stt1198)
- Barkhudaryan, L. V., Hakobyan, A. A., Karapetyan, A. G., et al. 2019, MNRAS, 490, 718, doi: [10.1093/mnras/stz2585](https://doi.org/10.1093/mnras/stz2585)
- Becerra, L., Rueda, J. A., Lorén-Aguilar, P., & García-Berro, E. 2018, ApJ, 857, 134, doi: [10.3847/1538-4357/aabc12](https://doi.org/10.3847/1538-4357/aabc12)
- Bédard, A., Bergeron, P., Brassard, P., & Fontaine, G. 2020, ApJ, 901, 93, doi: [10.3847/1538-4357/abafbe](https://doi.org/10.3847/1538-4357/abafbe)
- Blondin, S., Matheson, T., Kirshner, R. P., et al. 2012, AJ, 143, 126, doi: [10.1088/0004-6256/143/5/126](https://doi.org/10.1088/0004-6256/143/5/126)
- Boehner, P., Plewa, T., & Langer, N. 2017, MNRAS, 465, 2060, doi: [10.1093/mnras/stw2737](https://doi.org/10.1093/mnras/stw2737)
- Boos, S. J., Townsley, D. M., & Shen, K. J. 2024, arXiv e-prints, arXiv:2401.08011, doi: [10.48550/arXiv.2401.08011](https://doi.org/10.48550/arXiv.2401.08011)
- Boos, S. J., Townsley, D. M., Shen, K. J., Caldwell, S., & Miles, B. J. 2021, ApJ, 919, 126, doi: [10.3847/1538-4357/ac07a2](https://doi.org/10.3847/1538-4357/ac07a2)
- Briday, M., Rigault, M., Graziani, R., et al. 2022, A&A, 657, A22, doi: [10.1051/0004-6361/202141160](https://doi.org/10.1051/0004-6361/202141160)
- Burmeister, U. P., Ferrario, L., Pakmor, R., et al. 2023, MNRAS, 523, 527, doi: [10.1093/mnras/stad1394](https://doi.org/10.1093/mnras/stad1394)

Name	Bimodal?	Subtype	Host	$\log_{10} M_\star$ [dex]	$\log_{10} \text{SFR}$ [dex]
1981B	N	norm	NGC 4536	10.19 ± 0.10	0.47 ± 0.20
1986G	T	91bg	NGC 5128	10.92 ± 0.10	0.04 ± 0.20
1989B	N	norm	M 66	10.67 ± 0.10	0.50 ± 0.20
1990N	N	norm	NGC 4639	10.21 ± 0.10	-0.29 ± 0.20
1991T	N	91T	NGC 4527	10.66 ± 0.10	0.54 ± 0.20
1998aq	N	norm	NGC 3982	9.90 ± 0.10	0.14 ± 0.20
1998bu	N	norm	M 96	10.67 ± 0.10	-0.29 ± 0.20
1999aa	N	91T	NGC 2595	10.97 ± 0.14	0.57 ± 0.20
1999by	N	91bg	NGC 2841	10.93 ± 0.10	-0.07 ± 0.20
2000cx	N	norm	NGC 0524	10.99 ± 0.10	-0.56 ± 0.20
2002dj	N	norm	NGC 5018	10.95 ± 0.10	-0.63 ± 0.20
2002er	T	norm	UGC 10743	9.51 ± 0.10	-0.24 ± 0.20
2003du	N	norm	UGC 9391	8.73 ± 0.10	-0.99 ± 0.20
2003hv	Y	norm	NGC 1201	10.40 ± 0.20	-1.46 ± 0.20
2003gs	Y	91bg	NGC 0936	10.99 ± 0.10	-0.70 ± 0.20
2004bv	N	norm	NGC 6907	10.69 ± 0.11	0.92 ± 0.20
2004eo	N	norm	NGC 6928	11.18 ± 0.10	0.45 ± 0.20
2005am	Y	norm	NGC 2811	10.76 ± 0.10	-0.78 ± 0.20
2005cf	N	norm	MCG -01-39-003	9.40 ± 0.15	-0.50 ± 0.20
2007af	N	norm	NGC 5584	9.85 ± 0.13	0.02 ± 0.20
2007le	N	norm	NGC 7721	10.11 ± 0.10	-0.04 ± 0.20
2007on	Y	norm	NGC 1404	11.01 ± 0.10	-0.73 ± 0.20
2008Q	N	norm	NGC 0524	10.99 ± 0.10	-0.56 ± 0.20
2011by	N	norm	NGC 3972	9.71 ± 0.10	-0.68 ± 0.20
2011fe	N	norm	M 101	10.39 ± 0.10	0.54 ± 0.20
2011iv	Y	norm	NGC 1404	11.01 ± 0.10	-0.73 ± 0.20
2012cg	N	norm	NGC 4424	9.89 ± 0.10	-0.52 ± 0.20
2012fr	N	norm	NGC 1365	10.75 ± 0.10	1.15 ± 0.20
2012hr	N	norm	ESO 121-G026	10.52 ± 0.10	0.23 ± 0.20
2013aa	N	norm	NGC 5643	10.06 ± 0.10	0.33 ± 0.20
2013dy	N	norm	NGC 7250	8.97 ± 0.12	-0.40 ± 0.20
2013gy	N	norm	NGC 1418	10.21 ± 0.10	-0.36 ± 0.20
2014J	N	norm	M 82	10.01 ± 0.10	0.85 ± 0.20
2014bv	Y	norm	NGC 4386	10.52 ± 0.10	-1.16 ± 0.20
2015F	N	norm	NGC 2442	10.84 ± 0.10	0.64 ± 0.20
2015I	N	norm	NGC 2357	10.06 ± 0.10	-0.27 ± 0.20
2016coj	N	norm	NGC 4125	11.13 ± 0.10	-0.90 ± 0.20
2016fnr	N	norm	UGC 10502	10.70 ± 0.10	0.34 ± 0.20
2016iuh	T	91bg	UGC 07367	10.82 ± 0.10	-0.74 ± 0.20
2016gxp	N	91T	NGC 0051	9.70 ± 0.40	-0.20 ± 0.40
2017hjw	N	norm	UGC 03245	10.28 ± 0.10	0.08 ± 0.20
2017cbv	N	91T	NGC 5643	10.06 ± 0.10	0.33 ± 0.20
2017ckq	N	norm	ESO 437-G056	10.21 ± 0.10	-0.31 ± 0.20
2017erp	N	norm	NGC 5861	10.27 ± 0.10	0.55 ± 0.20
2017fzw	N	91bg	NGC 2217	10.96 ± 0.10	-0.15 ± 0.20
2018gv	N	norm	NGC 2525	9.87 ± 0.12	-0.04 ± 0.20
2018oh	N	norm	UGC 04780	9.32 ± 0.11	-0.44 ± 0.20
2018yu	N	norm	NGC 1888	11.01 ± 0.10	0.41 ± 0.20
ASASSN-14jg	N	norm	J2333-6034 ^a	9.80 ± 0.10	-0.29 ± 0.20
ASASSN-15uh	N	91T	KUG 0925+693	7.90 ± 0.35	-1.10 ± 0.35
ASASSN-16lx	N	norm	IC 0607	9.00 ± 0.35	-0.60 ± 0.35
ASASSN-17cz	N	norm	J1750-0148 ^b	9.30 ± 0.30	-0.50 ± 0.30
ASASSN-17pg	N	norm	NGC 3901	9.40 ± 0.10	-0.60 ± 0.20

Table 1. SN and host properties for the sample. Entries in the ‘Bimodal?’ column are one of: (Y)es, (N)o, or (T)entative.^aWISEA J233312.25-603420.6. ^bWISEA J175030.58-014802.8.

- Burns, C. R., Stritzinger, M., Phillips, M. M., et al. 2011, AJ, 141, 19, doi: [10.1088/0004-6256/141/1/19](https://doi.org/10.1088/0004-6256/141/1/19)
- Burns, C. R., Parent, E., Phillips, M. M., et al. 2018, ApJ, 869, 56, doi: [10.3847/1538-4357/aae51c](https://doi.org/10.3847/1538-4357/aae51c)
- Camacho-Neves, Y., Jha, S. W., Barna, B., et al. 2023, ApJ, 951, 67, doi: [10.3847/1538-4357/acd558](https://doi.org/10.3847/1538-4357/acd558)
- Carnall, A. C. 2017, arXiv e-prints, arXiv:1705.05165, doi: [10.48550/arXiv.1705.05165](https://doi.org/10.48550/arXiv.1705.05165)
- Carvalho, G. A., Anjos, R. C. d., Coelho, J. G., et al. 2022, ApJ, 940, 90, doi: [10.3847/1538-4357/ac9841](https://doi.org/10.3847/1538-4357/ac9841)
- Chakradhari, N. K., Sahu, D. K., & Anupama, G. C. 2019, MNRAS, 487, 1886, doi: [10.1093/mnras/stz1358](https://doi.org/10.1093/mnras/stz1358)
- Chamulak, D. A., Meakin, C. A., Seitenzahl, I. R., & Truran, J. W. 2012, ApJ, 744, 27, doi: [10.1088/0004-637X/744/1/27](https://doi.org/10.1088/0004-637X/744/1/27)
- Cheng, S., Cummings, J. D., Ménard, B., & Toonen, S. 2020, ApJ, 891, 160, doi: [10.3847/1538-4357/ab733c](https://doi.org/10.3847/1538-4357/ab733c)
- Childress, M., Aldering, G., Antilogus, P., et al. 2013, ApJ, 770, 108, doi: [10.1088/0004-637X/770/2/108](https://doi.org/10.1088/0004-637X/770/2/108)
- Chomiuk, L., Soderberg, A. M., Chevalier, R. A., et al. 2016, ApJ, 821, 119, doi: [10.3847/0004-637X/821/2/119](https://doi.org/10.3847/0004-637X/821/2/119)
- Collins, C. E., Gronow, S., Sim, S. A., & Röpke, F. K. 2022, MNRAS, 517, 5289, doi: [10.1093/mnras/stac2665](https://doi.org/10.1093/mnras/stac2665)
- Cronin, S. A., Utomo, D., Leroy, A. K., et al. 2021, ApJ, 923, 86, doi: [10.3847/1538-4357/ac28a2](https://doi.org/10.3847/1538-4357/ac28a2)
- Dan, M., Guillochon, J., Brüggen, M., Ramirez-Ruiz, E., & Rosswog, S. 2015, MNRAS, 454, 4411, doi: [10.1093/mnras/stv2289](https://doi.org/10.1093/mnras/stv2289)
- Dhawan, S., Leibundgut, B., Spyromilio, J., & Blondin, S. 2017, A&A, 602, A118, doi: [10.1051/0004-6361/201629793](https://doi.org/10.1051/0004-6361/201629793)
- Dong, S., Katz, B., Kushnir, D., & Prieto, J. L. 2015, MNRAS, 454, L61, doi: [10.1093/mnrasl/slv129](https://doi.org/10.1093/mnrasl/slv129)
- Dubay, L. O., Tucker, M. A., Do, A., Shappee, B. J., & Anand, G. S. 2022, ApJ, 926, 98, doi: [10.3847/1538-4357/ac3bb4](https://doi.org/10.3847/1538-4357/ac3bb4)
- Fang, X., Thompson, T. A., & Hirata, C. M. 2018, MNRAS, 476, 4234, doi: [10.1093/mnras/sty472](https://doi.org/10.1093/mnras/sty472)
- Fenn, D., Plewa, T., & Gawryszczak, A. 2016, MNRAS, 462, 2486, doi: [10.1093/mnras/stw1831](https://doi.org/10.1093/mnras/stw1831)
- Filippenko, A. V., Richmond, M. W., Branch, D., et al. 1992a, AJ, 104, 1543, doi: [10.1086/116339](https://doi.org/10.1086/116339)
- Filippenko, A. V., Richmond, M. W., Matheson, T., et al. 1992b, ApJL, 384, L15, doi: [10.1086/186252](https://doi.org/10.1086/186252)
- Foley, R. J., Jha, S. W., Pan, Y.-C., et al. 2016, MNRAS, 461, 433, doi: [10.1093/mnras/stw1320](https://doi.org/10.1093/mnras/stw1320)
- Foley, R. J., Challis, P. J., Chornock, R., et al. 2013, ApJ, 767, 57, doi: [10.1088/0004-637X/767/1/57](https://doi.org/10.1088/0004-637X/767/1/57)
- Foreman-Mackey, D., Hogg, D. W., Lang, D., & Goodman, J. 2013, PASP, 125, 306, doi: [10.1086/670067](https://doi.org/10.1086/670067)
- Gall, C., Stritzinger, M. D., Ashall, C., et al. 2018, A&A, 611, A58, doi: [10.1051/0004-6361/201730886](https://doi.org/10.1051/0004-6361/201730886)
- Garavini, G., Folatelli, G., Goobar, A., et al. 2004, AJ, 128, 387, doi: [10.1086/421747](https://doi.org/10.1086/421747)
- García-Senz, D., Cabezón, R. M., Arcones, A., Relaño, A., & Thielemann, F. K. 2013, MNRAS, 436, 3413, doi: [10.1093/mnras/stt1821](https://doi.org/10.1093/mnras/stt1821)
- Ginolin, M., Rigault, M., Copin, Y., et al. 2024, arXiv e-prints, arXiv:2406.02072, doi: [10.48550/arXiv.2406.02072](https://doi.org/10.48550/arXiv.2406.02072)
- Glanz, H., Perets, H. B., & Pakmor, R. 2023, arXiv e-prints, arXiv:2309.03300, doi: [10.48550/arXiv.2309.03300](https://doi.org/10.48550/arXiv.2309.03300)
- Graham, M. L., Kennedy, T. D., Kumar, S., et al. 2022, MNRAS, 511, 3682, doi: [10.1093/mnras/stac192](https://doi.org/10.1093/mnras/stac192)
- Gronow, S., Côté, B., Lach, F., et al. 2021, A&A, 656, A94, doi: [10.1051/0004-6361/202140881](https://doi.org/10.1051/0004-6361/202140881)
- Gupta, R. R., D’Andrea, C. B., Sako, M., et al. 2011, ApJ, 740, 92, doi: [10.1088/0004-637X/740/2/92](https://doi.org/10.1088/0004-637X/740/2/92)
- Hachinger, S., Mazzali, P. A., Taubenberger, S., Pakmor, R., & Hillebrandt, W. 2009, MNRAS, 399, 1238, doi: [10.1111/j.1365-2966.2009.15403.x](https://doi.org/10.1111/j.1365-2966.2009.15403.x)
- Hakobyan, A. A., Barkhudaryan, L. V., Karapetyan, A. G., et al. 2020, MNRAS, 499, 1424, doi: [10.1093/mnras/staa2940](https://doi.org/10.1093/mnras/staa2940)
- Hamers, A. S. 2018, MNRAS, 478, 620, doi: [10.1093/mnras/sty985](https://doi.org/10.1093/mnras/sty985)
- Hamers, A. S., Perets, H. B., Thompson, T. A., & Neunteufel, P. 2022, ApJ, 925, 178, doi: [10.3847/1538-4357/ac400b](https://doi.org/10.3847/1538-4357/ac400b)
- Harris, C. R., Millman, K. J., van der Walt, S. J., et al. 2020, Nature, 585, 357, doi: [10.1038/s41586-020-2649-2](https://doi.org/10.1038/s41586-020-2649-2)
- Hawley, W. P., Athanassiadou, T., & Timmes, F. X. 2012, ApJ, 759, 39, doi: [10.1088/0004-637X/759/1/39](https://doi.org/10.1088/0004-637X/759/1/39)
- Höflich, P., & Stein, J. 2002, ApJ, 568, 779, doi: [10.1086/338981](https://doi.org/10.1086/338981)
- Hoyle, F., & Fowler, W. A. 1960, ApJ, 132, 565, doi: [10.1086/146963](https://doi.org/10.1086/146963)
- Hunter, J. D. 2007, Computing in Science and Engineering, 9, 90, doi: [10.1109/MCSE.2007.55](https://doi.org/10.1109/MCSE.2007.55)
- Iben, I., J., & Tutukov, A. V. 1984, ApJS, 54, 335, doi: [10.1086/190932](https://doi.org/10.1086/190932)
- Iwamoto, K., Brachwitz, F., Nomoto, K., et al. 1999, ApJS, 125, 439, doi: [10.1086/313278](https://doi.org/10.1086/313278)
- Jha, S. W., Maguire, K., & Sullivan, M. 2019, Nature Astronomy, 3, 706, doi: [10.1038/s41550-019-0858-0](https://doi.org/10.1038/s41550-019-0858-0)
- Ji, S., Fisher, R. T., García-Berro, E., et al. 2013, ApJ, 773, 136, doi: [10.1088/0004-637X/773/2/136](https://doi.org/10.1088/0004-637X/773/2/136)
- Kang, Y., Lee, Y.-W., Kim, Y.-L., Chung, C., & Ree, C. H. 2020, ApJ, 889, 8, doi: [10.3847/1538-4357/ab5afc](https://doi.org/10.3847/1538-4357/ab5afc)

- Kasen, D. 2010, ApJ, 708, 1025, doi: [10.1088/0004-637X/708/2/1025](https://doi.org/10.1088/0004-637X/708/2/1025)
- Kelly, P. L., Hicken, M., Burke, D. L., Mandel, K. S., & Kirshner, R. P. 2010, ApJ, 715, 743, doi: [10.1088/0004-637X/715/2/743](https://doi.org/10.1088/0004-637X/715/2/743)
- Kelsey, L., Sullivan, M., Smith, M., et al. 2021, MNRAS, 501, 4861, doi: [10.1093/mnras/staa3924](https://doi.org/10.1093/mnras/staa3924)
- Kilic, M., Bergeron, P., Blouin, S., & Bédard, A. 2021, MNRAS, 503, 5397, doi: [10.1093/mnras/stab767](https://doi.org/10.1093/mnras/stab767)
- Kim, Y., Jordan, G. C., I., Graziani, C., et al. 2013, ApJ, 771, 55, doi: [10.1088/0004-637X/771/1/55](https://doi.org/10.1088/0004-637X/771/1/55)
- Kobayashi, C., Leung, S.-C., & Nomoto, K. 2020, ApJ, 895, 138, doi: [10.3847/1538-4357/ab8e44](https://doi.org/10.3847/1538-4357/ab8e44)
- Kushnir, D., Katz, B., Dong, S., Livne, E., & Fernández, R. 2013, ApJL, 778, L37, doi: [10.1088/2041-8205/778/2/L37](https://doi.org/10.1088/2041-8205/778/2/L37)
- Kwok, L. A., Jha, S. W., Temim, T., et al. 2023, ApJL, 944, L3, doi: [10.3847/2041-8213/acb4ec](https://doi.org/10.3847/2041-8213/acb4ec)
- Lampeitl, H., Smith, M., Nichol, R. C., et al. 2010, ApJ, 722, 566, doi: [10.1088/0004-637X/722/1/566](https://doi.org/10.1088/0004-637X/722/1/566)
- Larison, C., Jha, S. W., Kwok, L. A., & Camacho-Neves, Y. 2024, ApJ, 961, 185, doi: [10.3847/1538-4357/ad0e0f](https://doi.org/10.3847/1538-4357/ad0e0f)
- Leibundgut, B., Kirshner, R. P., Phillips, M. M., et al. 1993, AJ, 105, 301, doi: [10.1086/116427](https://doi.org/10.1086/116427)
- Leonard, D. C. 2007, ApJ, 670, 1275, doi: [10.1086/522367](https://doi.org/10.1086/522367)
- Leroy, A. K., Sandstrom, K. M., Lang, D., et al. 2019, ApJS, 244, 24, doi: [10.3847/1538-4365/ab3925](https://doi.org/10.3847/1538-4365/ab3925)
- Li, W., Filippenko, A. V., Chornock, R., et al. 2003, PASP, 115, 453, doi: [10.1086/374200](https://doi.org/10.1086/374200)
- Liu, Z.-W., Röpke, F. K., & Han, Z. 2023a, Research in Astronomy and Astrophysics, 23, 082001, doi: [10.1088/1674-4527/acd89e](https://doi.org/10.1088/1674-4527/acd89e)
- . 2023b, Research in Astronomy and Astrophysics, 23, 082001, doi: [10.1088/1674-4527/acd89e](https://doi.org/10.1088/1674-4527/acd89e)
- Livne, E. 1990, ApJL, 354, L53, doi: [10.1086/185721](https://doi.org/10.1086/185721)
- Maeda, K., Taubenberger, S., Sollerman, J., et al. 2010, ApJ, 708, 1703, doi: [10.1088/0004-637X/708/2/1703](https://doi.org/10.1088/0004-637X/708/2/1703)
- Maguire, K., Taubenberger, S., Sullivan, M., & Mazzali, P. A. 2016, MNRAS, 457, 3254, doi: [10.1093/mnras/stv2991](https://doi.org/10.1093/mnras/stv2991)
- Maguire, K., Sim, S. A., Shingles, L., et al. 2018, MNRAS, 477, 3567, doi: [10.1093/mnras/sty820](https://doi.org/10.1093/mnras/sty820)
- Maoz, D., Mannucci, F., & Nelemans, G. 2014, ARA&A, 52, 107, doi: [10.1146/annurev-astro-082812-141031](https://doi.org/10.1146/annurev-astro-082812-141031)
- Maoz, D., Sharon, K., & Gal-Yam, A. 2010, ApJ, 722, 1879, doi: [10.1088/0004-637X/722/2/1879](https://doi.org/10.1088/0004-637X/722/2/1879)
- Margutti, R., Soderberg, A. M., Chomiuk, L., et al. 2012, ApJ, 751, 134, doi: [10.1088/0004-637X/751/2/134](https://doi.org/10.1088/0004-637X/751/2/134)
- Marietta, E., Burrows, A., & Fryxell, B. 2000, ApJS, 128, 615, doi: [10.1086/313392](https://doi.org/10.1086/313392)
- Mattila, S., Lundqvist, P., Sollerman, J., et al. 2005, A&A, 443, 649, doi: [10.1051/0004-6361:20052731](https://doi.org/10.1051/0004-6361:20052731)
- Mazzali, P. A., Ashall, C., Pian, E., et al. 2018, MNRAS, 476, 2905, doi: [10.1093/mnras/sty434](https://doi.org/10.1093/mnras/sty434)
- Mazzali, P. A., Sullivan, M., Hachinger, S., et al. 2014, MNRAS, 439, 1959, doi: [10.1093/mnras/stu077](https://doi.org/10.1093/mnras/stu077)
- Meng, X., & Yang, W. 2012, A&A, 543, A137, doi: [10.1051/0004-6361/201218810](https://doi.org/10.1051/0004-6361/201218810)
- Meng, X.-C., Zhang, J.-J., Zhao, X., Li, L.-P., & Wang, X.-F. 2023, ApJ, 943, 159, doi: [10.3847/1538-4357/acad77](https://doi.org/10.3847/1538-4357/acad77)
- Morrell, N., Phillips, M. M., Folatelli, G., et al. 2024, ApJ, 967, 20, doi: [10.3847/1538-4357/ad38af](https://doi.org/10.3847/1538-4357/ad38af)
- Neopane, S., Bhargava, K., Fisher, R., et al. 2022, ApJ, 925, 92, doi: [10.3847/1538-4357/ac3b52](https://doi.org/10.3847/1538-4357/ac3b52)
- Newville, M., Stensitzki, T., Allen, D. B., & Ingargiola, A. 2014, LMFIT: Non-Linear Least-Square Minimization and Curve-Fitting for Python, 0.8.0, Zenodo, doi: [10.5281/zenodo.11813](https://doi.org/10.5281/zenodo.11813)
- Nomoto, K. 1982, ApJ, 253, 798, doi: [10.1086/159682](https://doi.org/10.1086/159682)
- Pakmor, R., Kromer, M., Röpke, F. K., et al. 2010, Nature, 463, 61, doi: [10.1038/nature08642](https://doi.org/10.1038/nature08642)
- Pakmor, R., Kromer, M., Taubenberger, S., et al. 2012, ApJL, 747, L10, doi: [10.1088/2041-8205/747/1/L10](https://doi.org/10.1088/2041-8205/747/1/L10)
- Pakmor, R., Kromer, M., Taubenberger, S., & Springel, V. 2013, ApJL, 770, L8, doi: [10.1088/2041-8205/770/1/L8](https://doi.org/10.1088/2041-8205/770/1/L8)
- Pakmor, R., Callan, F. P., Collins, C. E., et al. 2022, MNRAS, 517, 5260, doi: [10.1093/mnras/stac3107](https://doi.org/10.1093/mnras/stac3107)
- Pan, Y. C., Sullivan, M., Maguire, K., et al. 2015, MNRAS, 446, 354, doi: [10.1093/mnras/stu2121](https://doi.org/10.1093/mnras/stu2121)
- . 2014, MNRAS, 438, 1391, doi: [10.1093/mnras/stt2287](https://doi.org/10.1093/mnras/stt2287)
- Panagia, N., Van Dyk, S. D., Weiler, K. W., et al. 2006, ApJ, 646, 369, doi: [10.1086/504710](https://doi.org/10.1086/504710)
- Papish, O., & Perets, H. B. 2016, ApJ, 822, 19, doi: [10.3847/0004-637X/822/1/19](https://doi.org/10.3847/0004-637X/822/1/19)
- Papish, O., Soker, N., García-Berro, E., & Aznar-Siguán, G. 2015, MNRAS, 449, 942, doi: [10.1093/mnras/stv337](https://doi.org/10.1093/mnras/stv337)
- Pejcha, O., Antognini, J. M., Shappee, B. J., & Thompson, T. A. 2013, MNRAS, 435, 943, doi: [10.1093/mnras/stt1281](https://doi.org/10.1093/mnras/stt1281)
- Perets, H. B., Zenati, Y., Toonen, S., & Bobrick, A. 2019, arXiv e-prints, arXiv:1910.07532, doi: [10.48550/arXiv.1910.07532](https://doi.org/10.48550/arXiv.1910.07532)
- Phillips, M. M., Wells, L. A., Suntzeff, N. B., et al. 1992, AJ, 103, 1632, doi: [10.1086/116177](https://doi.org/10.1086/116177)
- Polin, A., Nugent, P., & Kasen, D. 2019, ApJ, 873, 84, doi: [10.3847/1538-4357/aafb6a](https://doi.org/10.3847/1538-4357/aafb6a)
- Raskin, C., Kasen, D., Moll, R., Schwab, J., & Woosley, S. 2014, ApJ, 788, 75, doi: [10.1088/0004-637X/788/1/75](https://doi.org/10.1088/0004-637X/788/1/75)

- Raskin, C., Scannapieco, E., Rockefeller, G., et al. 2010, ApJ, 724, 111, doi: [10.1088/0004-637X/724/1/111](https://doi.org/10.1088/0004-637X/724/1/111)
- Raskin, C., Timmes, F. X., Scannapieco, E., Diehl, S., & Fryer, C. 2009, MNRAS, 399, L156, doi: [10.1111/j.1745-3933.2009.00743.x](https://doi.org/10.1111/j.1745-3933.2009.00743.x)
- Rigault, M., Copin, Y., Aldering, G., et al. 2013, A&A, 560, A66, doi: [10.1051/0004-6361/201322104](https://doi.org/10.1051/0004-6361/201322104)
- Rigault, M., Brinnel, V., Aldering, G., et al. 2020, A&A, 644, A176, doi: [10.1051/0004-6361/201730404](https://doi.org/10.1051/0004-6361/201730404)
- Roman, M., Hardin, D., Betoule, M., et al. 2018, A&A, 615, A68, doi: [10.1051/0004-6361/201731425](https://doi.org/10.1051/0004-6361/201731425)
- Rosswog, S., Kasen, D., Guillochon, J., & Ramirez-Ruiz, E. 2009, ApJL, 705, L128, doi: [10.1088/0004-637X/705/2/L128](https://doi.org/10.1088/0004-637X/705/2/L128)
- Salim, S., Lee, J. C., Janowiecki, S., et al. 2016, ApJS, 227, 2, doi: [10.3847/0067-0049/227/1/2](https://doi.org/10.3847/0067-0049/227/1/2)
- Scalzo, R. A., Parent, E., Burns, C., et al. 2019, MNRAS, 483, 628, doi: [10.1093/mnras/sty3178](https://doi.org/10.1093/mnras/sty3178)
- Schaefer, B. E., & Pagnotta, A. 2012, Nature, 481, 164, doi: [10.1038/nature10692](https://doi.org/10.1038/nature10692)
- Seitenzahl, I. R., Meakin, C. A., Townsley, D. M., Lamb, D. Q., & Truran, J. W. 2009, ApJ, 696, 515, doi: [10.1088/0004-637X/696/1/515](https://doi.org/10.1088/0004-637X/696/1/515)
- Seitenzahl, I. R., & Townsley, D. M. 2017, in Handbook of Supernovae, ed. A. W. Alsabti & P. Murdin, 1955, doi: [10.1007/978-3-319-21846-5_87](https://doi.org/10.1007/978-3-319-21846-5_87)
- Seitenzahl, I. R., Ciaraldi-Schoolmann, F., Röpke, F. K., et al. 2013, MNRAS, 429, 1156, doi: [10.1093/mnras/sts402](https://doi.org/10.1093/mnras/sts402)
- Shappee, B. J., Piro, A. L., Stanek, K. Z., et al. 2018, ApJ, 855, 6, doi: [10.3847/1538-4357/aaa1e9](https://doi.org/10.3847/1538-4357/aaa1e9)
- Shappee, B. J., & Thompson, T. A. 2013, ApJ, 766, 64, doi: [10.1088/0004-637X/766/1/64](https://doi.org/10.1088/0004-637X/766/1/64)
- Shen, K. J., Boos, S. J., Townsley, D. M., & Kasen, D. 2021, ApJ, 922, 68, doi: [10.3847/1538-4357/ac2304](https://doi.org/10.3847/1538-4357/ac2304)
- Shen, K. J., & Moore, K. 2014, ApJ, 797, 46, doi: [10.1088/0004-637X/797/1/46](https://doi.org/10.1088/0004-637X/797/1/46)
- Shen, K. J., Boubert, D., Gänsicke, B. T., et al. 2018, ApJ, 865, 15, doi: [10.3847/1538-4357/aad55b](https://doi.org/10.3847/1538-4357/aad55b)
- Silverman, J. M., Foley, R. J., Filippenko, A. V., et al. 2012a, MNRAS, 425, 1789, doi: [10.1111/j.1365-2966.2012.21270.x](https://doi.org/10.1111/j.1365-2966.2012.21270.x)
- Silverman, J. M., Ganeshalingam, M., Cenko, S. B., et al. 2012b, ApJL, 756, L7, doi: [10.1088/2041-8205/756/1/L7](https://doi.org/10.1088/2041-8205/756/1/L7)
- Smith, M., Nichol, R. C., Dilday, B., et al. 2012, ApJ, 755, 61, doi: [10.1088/0004-637X/755/1/61](https://doi.org/10.1088/0004-637X/755/1/61)
- Sullivan, M., Conley, A., Howell, D. A., et al. 2010, MNRAS, 406, 782, doi: [10.1111/j.1365-2966.2010.16731.x](https://doi.org/10.1111/j.1365-2966.2010.16731.x)
- Tanikawa, A., Nomoto, K., Nakasato, N., & Maeda, K. 2019, ApJ, 885, 103, doi: [10.3847/1538-4357/ab46b6](https://doi.org/10.3847/1538-4357/ab46b6)
- Taubenberger, S., Hachinger, S., Pignata, G., et al. 2008, MNRAS, 385, 75, doi: [10.1111/j.1365-2966.2008.12843.x](https://doi.org/10.1111/j.1365-2966.2008.12843.x)
- The pandas development Team. 2024, pandas-dev/pandas: Pandas, v2.2.2, Zenodo, doi: [10.5281/zenodo.3509134](https://doi.org/10.5281/zenodo.3509134)
- Thompson, T. A. 2011, ApJ, 741, 82, doi: [10.1088/0004-637X/741/2/82](https://doi.org/10.1088/0004-637X/741/2/82)
- Toonen, S., Perets, H. B., & Hamers, A. S. 2018, A&A, 610, A22, doi: [10.1051/0004-6361/201731874](https://doi.org/10.1051/0004-6361/201731874)
- Tucker, M. A., & Shappee, B. J. 2024, ApJ, 962, 74, doi: [10.3847/1538-4357/ad1b4e](https://doi.org/10.3847/1538-4357/ad1b4e)
- Tucker, M. A., Shappee, B. J., Valletty, P. J., et al. 2020, MNRAS, 493, 1044, doi: [10.1093/mnras/stz3390](https://doi.org/10.1093/mnras/stz3390)
- Tutukov, A. V., & Yungelson, L. R. 1979, AcA, 29, 665
- Valley, P. J., Tucker, M. A., Shappee, B. J., et al. 2020, MNRAS, 492, 3553, doi: [10.1093/mnras/staa003](https://doi.org/10.1093/mnras/staa003)
- van der Walt, S., Colbert, S. C., & Varoquaux, G. 2011, Computing in Science and Engineering, 13, 22, doi: [10.1109/MCSE.2011.37](https://doi.org/10.1109/MCSE.2011.37)
- van Rossum, D. R., Kashyap, R., Fisher, R., et al. 2016, ApJ, 827, 128, doi: [10.3847/0004-637X/827/2/128](https://doi.org/10.3847/0004-637X/827/2/128)
- Virtanen, P., Gommers, R., Oliphant, T. E., et al. 2020, Nature Methods, 17, 261, doi: [10.1038/s41592-019-0686-2](https://doi.org/10.1038/s41592-019-0686-2)
- Wang, X., Wang, L., Filippenko, A. V., Zhang, T., & Zhao, X. 2013, Science, 340, 170, doi: [10.1126/science.1231502](https://doi.org/10.1126/science.1231502)
- Wheeler, J. C., Lecar, M., & McKee, C. F. 1975, ApJ, 200, 145, doi: [10.1086/153771](https://doi.org/10.1086/153771)
- Whelan, J., & Iben, Icko, J. 1973, ApJ, 186, 1007, doi: [10.1086/152565](https://doi.org/10.1086/152565)
- Wilk, K. D., Hillier, D. J., & Dessart, L. 2020, MNRAS, 494, 2221, doi: [10.1093/mnras/staa640](https://doi.org/10.1093/mnras/staa640)
- Wiseman, P., Sullivan, M., Smith, M., & Popovic, B. 2023, MNRAS, 520, 6214, doi: [10.1093/mnras/stad488](https://doi.org/10.1093/mnras/stad488)
- Wiseman, P., Vincenzi, M., Sullivan, M., et al. 2022, MNRAS, 515, 4587, doi: [10.1093/mnras/stac1984](https://doi.org/10.1093/mnras/stac1984)
- Wu, C., Xiong, H., & Wang, X. 2022, MNRAS, 512, 2972, doi: [10.1093/mnras/stac273](https://doi.org/10.1093/mnras/stac273)
- Yoshida, S. 2021, ApJ, 906, 29, doi: [10.3847/1538-4357/abc7bd](https://doi.org/10.3847/1538-4357/abc7bd)
- Yu, H., Weinberg, N. N., & Fuller, J. 2020, MNRAS, 496, 5482, doi: [10.1093/mnras/staa1858](https://doi.org/10.1093/mnras/staa1858)
- Yungelson, L. R., & Kuranov, A. G. 2017, MNRAS, 464, 1607, doi: [10.1093/mnras/stw2432](https://doi.org/10.1093/mnras/stw2432)
- Zou, Z.-C., Zhou, X.-L., & Huang, Y.-F. 2020, Research in Astronomy and Astrophysics, 20, 137, doi: [10.1088/1674-4527/20/9/137](https://doi.org/10.1088/1674-4527/20/9/137)